

S.C. Buranay^{1,*}, N. Arshad²¹*Eastern Mediterranean University, Famagusta, North Cyprus, Turkey;*²*Rauf Denktas University, Nicosia, North Cyprus, Turkey**(E-mail: suzan.buranay@emu.edu.tr, nouman.arshad@rdu.edu.tr)*

Solution of heat equation by a novel implicit scheme using block hybrid preconditioning of the conjugate gradient method

The main goal of the study is the approximation of the solution to the Dirichlet boundary value problem (DBVP) of the heat equation on a rectangle by developing a new difference method on a grid system of hexagons. It is proved that the given special scheme is unconditionally stable and converges to the exact solution on the grids with fourth order accuracy in space variables and second order accuracy in time variable. Secondly, an incomplete block factorization is given for symmetric positive definite block tridiagonal (SPD-BT) matrices utilizing a conservative iterative method that approximates the inverse of the pivoting diagonal blocks by preserving the symmetric positive definite property. Subsequently, by using this factorization block hybrid preconditioning of the conjugate gradient (BHP-CG) method is applied to solve the obtained algebraic system of equations at each time level.

Keywords: Heat equation, implicit scheme, hexagonal grid, stability analysis, symmetric positive definite matrix, approximate inverse, incomplete block factorization, block hybrid preconditioning, conjugate gradient method.

Introduction

For many mathematical models, especially partial differential equations (PDEs), their analytical solutions are not available. Therefore, for computing the approximate solutions economical and stable numerical algorithms based on effective theoretical results are getting more important as more advanced computers are designed.

Among some numerical methods for approximating the solutions of PDEs, the finite difference method is a widely used approach and the construction of stable and time efficient schemes are essential. Recent advances in finite difference methods for solving PDEs include [1–7].

More than a half century ago, in 1967, the approximation of the pure diffusion equation

$$\frac{\partial u}{\partial t} = \frac{\partial^2 u}{\partial x_1^2} + \frac{\partial^2 u}{\partial x_2^2},$$

on regular hexagonal grids was analyzed by giving two implicit difference schemes, defined on three layers with 21-point and on two layers with 14-point both with fourth order accuracy in space and second order accuracy in time [8].

Since then, the applicability of the hexagonal grids in many branches of science has been investigated. Among them is the research on eligibility of the icosahedral-hexagonal grids in meteorological applications. Finite difference schemes on a spherical geodesic grid were given to integrate the barotropic vorticity equation [9,10]. Further, the hexagonal grid was extended to the integration of the primitive equations of fluid dynamics [11–13]. Later, an integration scheme of the primitive equation model by using on icosahedral-hexagonal grid system with an application to the shallow water equation was given [14]. Additionally, for the simulations of oscillations in shallow circular basins, finite difference techniques

*Corresponding author.

E-mail: suzan.buranay@emu.edu.tr

on the irregular grids were analyzed [15]. Furthermore, hexagonal grids were used for the simulation of atmospheric processes [16].

Nowadays, the investigation of triangular and hexagonal system of grids has gained more interest in engineering, applied sciences, computer science, natural sciences and in environmental sciences. Such as the numerical solution of boundary value problems of PDEs using finite difference method in convection diffusion equation [17], in the Laplace equation [18], and in the heat equation [5], and derivatives of the solution to the heat equation [6, 7]. Additionally, hexagonal grids were also used in finite volume method [19]. For digital image processing and graph processing, some examples include [20] where digitized rotations of 12 neighbors on the triangular grid were given by considering more general setting especially the midpoint, the corner points and the edge midpoints as rotation centers. Also, in [21] the bijectivity of the digitized rotations for the closest neighbors in rectangular, triangular and hexagonal grids were compared. In addition, the firefighter problem, which is an iterative graph process, was studied on hexagonal grids in [22]. For hydrologic modelling, we mention the study by [23] in which a watershed delineation model using the hexagonal grid spatial discretization method was developed.

The contributions of this work can be summarised as: the DBVP of the heat equation

$$\frac{\partial u}{\partial t} = \omega \left(\frac{\partial^2 u}{\partial x_1^2} + \frac{\partial^2 u}{\partial x_2^2} \right) - bu + f(x_1, x_2, t), \quad (1)$$

given on a rectangle D where $\omega > 0, b \geq 0$ are constants is considered. A new difference method of order of convergence $O(h^4 + \tau^2)$ with 14-point on two layers constructed on hexagonal grids is proposed. Here, the increments in the variables x_1 and x_2 are denoted by h and $\frac{\sqrt{3}}{2}h$ accordingly and τ denotes the increment in time. Further, the unconditional stability of the given scheme is shown. Furthermore, for SPD-BT matrices an incomplete block matrix factorization algorithm is developed. At each stage of the recursion for approximating the pivoting diagonal block matrix inverses, the constructed algorithm uses a two step iterative method with very high rate of convergence (order 33 see [24]). It is proven that at each iteration the pivoting diagonal block matrix and its approximate inverse are symmetric positive definite (SPD) matrices. Subsequently this factorization and the pivoting block approximate inverses are used to precondition the conjugate gradient method [25], which we call block hybrid preconditioning of the conjugate gradient (BHP-CG) method.

1 DBVP of the heat equation and discretization

We take the rectangle $D = \{x = (x_1, x_2) : 0 < x_1 < a_1, 0 < x_2 < a_2\}$. We denote its sides by $v_j, j = 1, 2, 3, 4$ and its boundary by $S = \bigcup_{j=1}^4 v_j$, so that $\bar{D} = D \cup S$ is the closure of D . Let $Q_T = D \times (0, T)$, and indicate the lateral surface by $S_T = \{(x, t), x \in S, t \in [0, T]\}$ and the closure of Q_T by \bar{Q}_T . We consider the DBVP of heat equation in (1)

$$\frac{\partial u}{\partial t} = \omega \left(\frac{\partial^2 u}{\partial x_1^2} + \frac{\partial^2 u}{\partial x_2^2} \right) - bu + f(x_1, x_2, t) \text{ on } Q_T, \quad (2)$$

$$u(x_1, x_2, 0) = \varphi(x_1, x_2) \text{ on } \bar{D}, \quad (3)$$

$$u(x_1, x_2, t) = \phi(x_1, x_2, t) \text{ on } S_T, \quad (4)$$

where $\omega > 0$ and $b \geq 0$ are constant. In this study, further investigations are given with the assumption that DBVP in (2)–(4) has the unique solution u from the Hölder space $C_{x,t}^{6+\alpha, 3+\frac{\alpha}{2}}(\bar{Q}_T), 0 < \alpha < 1$.

1.1 Implicit scheme on rectangular grids

First we consider the classical rectangular grid approximation of the problem (2)–(4) when the value of the constant $b = 0$ in Equation (2). We take the step sizes $h_1 = \frac{a_1}{M_1}$ and $h_2 = \frac{a_2}{M_2}$ where, M_1 and M_2 are positive integers. Further, the set of rectangular grids on D is defined as

$$D^{h_1, h_2} = \{x = (x_1, x_2) \in D : x_i = l_i h_i, l_i = 1, 2, \dots, M_i - 1, i = 1, 2\}.$$

Let S^{h_1, h_2} be the set of rectangular grid points on S and $\overline{D^{h_1, h_2}} = D^{h_1, h_2} \cup S^{h_1, h_2}$. Further let,

$$\begin{aligned} \gamma_\tau &= \left\{ t_k = k\tau, \tau = \frac{T}{M'}, k = 1, \dots, M' \right\}, \\ \bar{\gamma}_\tau &= \left\{ t_k = k\tau, \tau = \frac{T}{M'}, k = 0, \dots, M' \right\}. \end{aligned}$$

Also

$$\begin{aligned} D^{h_1, h_2} \gamma_\tau &= D^{h_1, h_2} \times \gamma_\tau = \left\{ (x, t) : x \in D^{h_1, h_2}, t \in \gamma_\tau \right\}, \\ S_T^{h_1, h_2} &= S^{h_1, h_2} \times \bar{\gamma}_\tau = \left\{ (x, t) : x \in S^{h_1, h_2}, t \in \bar{\gamma}_\tau \right\}. \end{aligned}$$

The following unconditionally stable 14-point implicit method on rectangular grids is considered [26]. Rectangular Difference Problem (RDP)

$$\begin{aligned} \Gamma u_{h, \tau} &= \omega \sigma_1 \Lambda_1 u_{h, \tau}^{k+1} + \omega (1 - \sigma_1) \Lambda_1 u_{h, \tau}^k + \omega \sigma_2 \Lambda_2 u_{h, \tau}^{k+1} + \omega (1 - \sigma_2) \Lambda_2 u_{h, \tau}^k \\ &+ \omega \frac{h_1^2 + h_2^2}{12} \Lambda_1 \Lambda_2 u_{h, \tau}^k + \beta \text{ on } D^{h_1, h_2} \gamma_\tau, \end{aligned} \tag{5}$$

$$u_{h, \tau} = \varphi(x_1, x_2), t = 0 \text{ on } \overline{D^{h_1, h_2}}, \tag{6}$$

$$u_{h, \tau} = \phi(x_1, x_2, t) \text{ on } S_T^{h_1, h_2}, \tag{7}$$

where

$$\begin{aligned} \sigma_1 &= \frac{1}{2} - \frac{h_1^2}{12\tau}, \quad \sigma_2 = \frac{1}{2} - \frac{h_2^2}{12\tau}, \\ \Gamma u &= \frac{u(x_1, x_2, t + \tau) - u(x_1, x_2, t)}{\tau}, \\ \Lambda_1 u^k &= [u(x_1 + h_1, x_2, t) - 2u(x_1, x_2, t) + u(x_1 - h_1, x_2, t)] / h_1^2, \\ \Lambda_2 u^k &= [u(x_1, x_2 + h_2, t) - 2u(x_1, x_2, t) + u(x_1, x_2 - h_2, t)] / h_2^2, \\ \beta &= f_{P_0}^{k+\frac{1}{2}} + \frac{h_1^2}{12} \Lambda_1 f_{P_0}^{k+\frac{1}{2}} + \frac{h_2^2}{12} \Lambda_2 f_{P_0}^{k+\frac{1}{2}}, \end{aligned}$$

and $f_{P_0}^{k+\frac{1}{2}} = f(x_1, x_2, t + \frac{\tau}{2})$. The scheme has the order of accuracy $O\left(|\hat{h}|^4 + \tau^2\right)$. Here, $|\hat{h}| = \sqrt{h_1^2 + h_2^2}$ and we denote the system (5)–(7) by

$$\tilde{K}_1 U^{k+1} = \tilde{K}_2 U^k + \tau \tilde{F}^{k*}, \tag{8}$$

where \tilde{K}_1, \tilde{K}_2 are real block tridiagonal matrices with 5 nonzero and 9 nonzero diagonals, respectively. The vector \tilde{F}^{k*} is computed from the initial and boundary function values and the heat source function f .

1.2 Novel implicit scheme on hexagonal grids

Let N_1 be a positive integer and $h = a_1/N_1 > 0$. For the ease of explanation of the new scheme we assume that a_2 is multiple of $\sqrt{3}$. Using the step size h we assign a hexagonal grid on D and denote this set by D^h as

$$D^h = \left\{ x = (x_1, x_2) \in D : x_1 = \frac{p-q}{2}h, x_2 = \frac{\sqrt{3}(p+q)}{2}h, \right. \\ \left. p = 1, 2, \dots, q = 0 \pm 1 \pm 2, \dots \right\}.$$

Further $\overline{D^h}$ is the closure of D^h . In addition, P_0 is the center and $P_i, i = 1, \dots, 6$ are the neighboring points in the pattern $Patt(P_0)$ of the hexagon. The set of interior nodes are categorized as regular and irregular hexagons. Those hexagons with $Patt(P_0) \in \overline{D^h}$ are called regular and those with a center P_0 that lies $\frac{h}{2}$ units away from the boundary are called irregular hexagons. The set of irregular hexagons with a left ghost point are denoted by D^{*lh} and those with a right ghost point are presented by D^{*rh} . Also, $D^{*h} = D^{*lh} \cup D^{*rh}$ and $D^{0h} = D^h \setminus D^{*h}$. Table 1 presents the function values of u, f and the second order pure derivatives of f . In this table, if $P_0 \in D^{*lh} \gamma_\tau$ then the value of $\hat{s} = 0$ and if $P_0 \in D^{*rh} \gamma_\tau$ then $\hat{s} = a_1$. Besides $k+l, l = 0, \frac{1}{2}, 1$ denote the time levels $t = (k+l)\tau$ for $k = 0, 1, \dots, M' - 1$. Furthermore, the numerical solution on hexagonal grid system is presented by $u_{h,\tau,P_i}^{k+1}, i = 0, \dots, 6$, and at boundary points by u_{h,τ,P_A}^{k+1} , when $t = (k+1)\tau$, for $k = 0, 1, \dots, M' - 1$. Figure 1 illustrates the irregular hexagons and the exact solution at the center and the neighbouring points of the pattern at $t = k\tau$ and $(k+1)\tau$ time levels.

Table 1

Notations used to denote the function values.

$u_{P_0}^{k+1} = u(x_1, x_2, t + \tau)$	$u_{P_A}^{k+1} = u(\hat{s}, x_2, t + \tau)$
$u_{P_1}^{k+1} = u(x_1 - \frac{h}{2}, x_2 + \frac{\sqrt{3}}{2}h, t + \tau)$	$f_{P_0}^{k+\frac{1}{2}} = f(x_1, x_2, t + \frac{\tau}{2})$
$u_{P_2}^{k+1} = u(x_1 - h, x_2, t + \tau)$	$f_{P_A}^{k+1} = f(\hat{s}, x_2, t + \tau)$
$u_{P_3}^{k+1} = u(x_1 - \frac{h}{2}, x_2 - \frac{\sqrt{3}}{2}h, t + \tau)$	$f_{P_A}^{k+\frac{1}{2}} = f(\hat{s}, x_2, t + \frac{\tau}{2})$
$u_{P_4}^{k+1} = u(x_1 + \frac{h}{2}, x_2 - \frac{\sqrt{3}}{2}h, t + \tau)$	$f_{P_A}^k = f(\hat{s}, x_2, t)$
$u_{P_5}^{k+1} = u(x_1 + h, x_2, t + \tau)$	$\partial_{x_1}^2 f_{P_0}^{k+\frac{1}{2}} = \frac{\partial^2 f}{\partial x_1^2} \Big _{(x_1, x_2, t + \frac{\tau}{2})}$
$u_{P_6}^{k+1} = u(x_1 + \frac{h}{2}, x_2 + \frac{\sqrt{3}}{2}h, t + \tau)$	$\partial_{x_2}^2 f_{P_0}^{k+\frac{1}{2}} = \frac{\partial^2 f}{\partial x_2^2} \Big _{(x_1, x_2, t + \frac{\tau}{2})}$

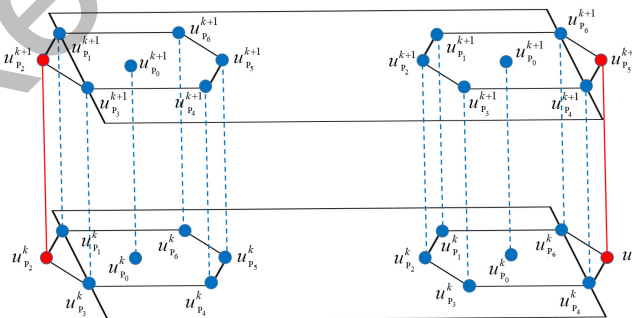


Figure 1. The illustration of the irregular hexagons and the solution for two time echelons.

Also on the hexagon system of grids we present the set of hexagonal grids on S by S^h and the sets

$$D^h \gamma_\tau = D^h \times \gamma_\tau = \left\{ (x, t) : x \in D^h, t \in \gamma_\tau \right\}, \\ S_T^h = S^h \times \bar{\gamma}_\tau = \left\{ (x, t) : x \in S^h, t \in \bar{\gamma}_\tau \right\},$$

present interior, and lateral surface nodes respectively. Let $D^{*lh}\gamma_\tau = D^{*lh} \times \gamma_\tau \subset D^h\gamma_\tau$ and $D^{*rh}\gamma_\tau = D^{*rh} \times \gamma_\tau \subset D^h\gamma_\tau$ and $D^{*h}\gamma_\tau = D^{*lh}\gamma_\tau \cup D^{*rh}\gamma_\tau$, also $D^{0h}\gamma_\tau = D^h\gamma_\tau \setminus D^{*h}\gamma_\tau$. Figure 2 shows the hexagonal grid covering of the rectangle D for three time echelons $t - \tau, t$ and $t + \tau$, on which the ghost points are denoted by red colour.

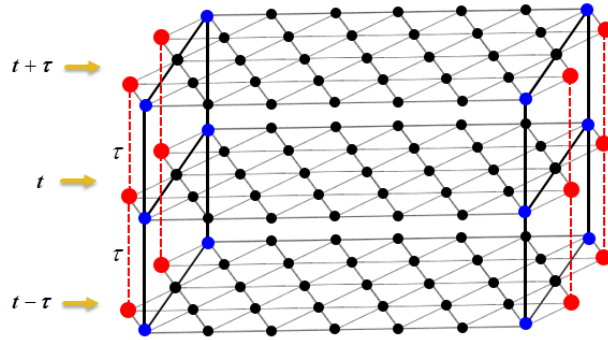


Figure 2. Hexagonal grid covering of the rectangle D for three time echelons $t - \tau, t$ and $t + \tau$.

We propose the next difference problem on hexagon system of grids to approximate the solution of the DBVP in (2)–(4).

Hexagonal Difference Problem (HDP)

$$\Theta_{h,\tau}^1 u_{h,\tau}^{k+1} = \Lambda_{h,\tau}^1 u_{h,\tau}^k + \psi^1 \text{ on } D^{0h}\gamma_\tau, \tag{9}$$

$$\Theta_{h,\tau}^2 u_{h,\tau}^{k+1} = \Lambda_{h,\tau}^2 u_{h,\tau}^k + E_{h,\tau}\phi + \psi^2 \text{ on } D^{*h}\gamma_\tau, \tag{10}$$

$$u_{h,\tau} = \varphi(x_1, x_2) \text{ on } t = 0, \overline{D^h}, \tag{11}$$

$$u_{h,\tau} = \phi(x_1, x_2, t) \text{ on } S_T^h, \tag{12}$$

$k = 1, 2, \dots, M' - 1$, where

$$\psi^1 = f_{P_0}^{k+\frac{1}{2}} + \frac{1}{16}h^2 \left(\partial_{x_1}^2 f_{P_0}^{k+\frac{1}{2}} + \partial_{x_2}^2 f_{P_0}^{k+\frac{1}{2}} \right), \tag{13}$$

$$\begin{aligned} \psi^2 = & \frac{h^2}{96\tau\omega} \left(f_{P_A}^{k+1} - f_{P_A}^k \right) - \left(\frac{1}{6} - \frac{h^2b}{96\omega} \right) f_{P_A}^{k+\frac{1}{2}} + f_{P_0}^{k+\frac{1}{2}} \\ & + \frac{1}{16}h^2 \left(\partial_{x_1}^2 f_{P_0}^{k+\frac{1}{2}} + \partial_{x_2}^2 f_{P_0}^{k+\frac{1}{2}} \right), \end{aligned} \tag{14}$$

$$\Theta_{h,\tau}^1 u^{k+1} = \left(\frac{3}{4\tau} + \frac{2\omega}{h^2} + \frac{3}{8}b \right) u_{P_0}^{k+1} + \left(\frac{1}{24\tau} - \frac{\omega}{3h^2} + \frac{b}{48} \right) \sum_{i=1}^6 u_{P_i}^{k+1}, \tag{15}$$

$$\Lambda_{h,\tau}^1 u^k = \left(\frac{3}{4\tau} - \frac{2\omega}{h^2} - \frac{3}{8}b \right) u_{P_0}^k + \left(\frac{1}{24\tau} + \frac{\omega}{3h^2} - \frac{b}{48} \right) \sum_{i=1}^6 u_{P_i}^k, \tag{16}$$

$$\begin{aligned} \Theta_{h,\tau}^2 u^{k+1} = & \left(\frac{17}{24\tau} + \frac{7\omega}{3h^2} + \frac{17}{48}b \right) u_{P_0}^{k+1} + \left(\frac{1}{24\tau} - \frac{\omega}{3h^2} + \frac{b}{48} \right) \left(u(s + \eta, x_2, t + \tau) \right. \\ & \left. + u\left(s, x_2 + \frac{\sqrt{3}}{2}h, t + \tau\right) + u\left(s, x_2 - \frac{\sqrt{3}}{2}h, t + \tau\right) \right), \end{aligned}$$

$$\begin{aligned}
 E_{h,\tau}\phi &= \left(-\frac{1}{36\tau} + \frac{2\omega}{9h^2} - \frac{b}{72}\right) \left(\phi(\widehat{s}, x_2 + \frac{\sqrt{3}}{2}h, t + \tau) + \phi(\widehat{s}, x_2 - \frac{\sqrt{3}}{2}h, t + \tau)\right) \\
 &+ \left(\frac{1}{36\tau} + \frac{2\omega}{9h^2} - \frac{b}{72}\right) \left(\phi(\widehat{s}, x_2 + \frac{\sqrt{3}}{2}h, t) + \phi(\widehat{s}, x_2 - \frac{\sqrt{3}}{2}h, t)\right) \\
 &+ \left(\frac{1}{18\tau} + \frac{8\omega}{9h^2} - \frac{h^2b}{48\omega\tau} + \frac{b}{36} - \frac{h^2b^2}{192\omega}\right) \phi(\widehat{s}, x_2, t + \tau) \\
 &- \left(\frac{1}{18\tau} - \frac{8\omega}{9h^2} - \frac{h^2b}{48\omega\tau} - \frac{b}{36} + \frac{h^2b^2}{192\omega}\right) \phi(\widehat{s}, x_2, t), \\
 \Lambda_{h,\tau}^2 u^k &= \left(\frac{17}{24\tau} - \frac{7\omega}{3h^2} - \frac{17}{48}b\right) u_{P_0}^k + \left(\frac{1}{24\tau} + \frac{\omega}{3h^2} - \frac{b}{48}\right) \left(u(s, x_2 + \frac{\sqrt{3}}{2}h, t) \right. \\
 &\quad \left. + u(s, x_2 - \frac{\sqrt{3}}{2}h, t) + u(s + \eta, x_2, t)\right),
 \end{aligned}$$

and

$$\begin{aligned}
 &\text{if } P_0 \in D^{*lh}\gamma_\tau, \text{ then } s = h, \widehat{s} = 0, \eta = \frac{h}{2}. \\
 &\text{if } P_0 \in D^{*rh}\gamma_\tau, \text{ then } s = a_1 - h, \widehat{s} = a_1, \eta = -\frac{h}{2}.
 \end{aligned}$$

2 Analysis of HDP (9)-(12)

First we analyze the approximation order of the special scheme in HDP (9)–(12).

Theorem 1. The scheme HDP (9)–(12) has the approximation order $O(h^4 + \tau^2)$.

Proof. Let $(x_1, x_2, t + \tau)$ and $(x_1, x_2, t) \in D^h\gamma_\tau$ be the centers (P_0) of the hexagons at time moment $(k + 1)\tau$ and $k\tau$ respectively for $k = 0, \dots, M' - 1$. From Equation (9) and using (13), (15) and (16) for regular hexagonal grids the scheme is

$$\begin{aligned}
 &\frac{3}{4} \frac{u_{h,\tau,P_0}^{k+1} - u_{h,\tau,P_0}^k}{\tau} + \frac{1}{24} \sum_{i=1}^6 \frac{u_{h,\tau,P_i}^{k+1} - u_{h,\tau,P_i}^k}{\tau} \\
 &= \frac{\omega}{3h^2} \left(\sum_{i=1}^6 u_{h,\tau,P_i}^{k+1} - 6u_{h,\tau,P_0}^{k+1}\right) + \frac{\omega}{3h^2} \left(\sum_{i=1}^6 u_{h,\tau,P_i}^k - 6u_{h,\tau,P_0}^k\right) \\
 &\quad - \frac{b}{48} \sum_{i=1}^6 u_{h,\tau,P_i}^{k+1} - \frac{3}{8}bu_{h,\tau,P_0}^{k+1} - \frac{b}{48} \sum_{i=1}^6 u_{h,\tau,P_i}^k - \frac{3}{8}bu_{h,\tau,P_0}^k \\
 &\quad + f_{P_0}^{k+\frac{1}{2}} + \frac{1}{16}h^2 \left(\partial_{x_1}^2 f_{P_0}^{k+\frac{1}{2}} + \partial_{x_2}^2 f_{P_0}^{k+\frac{1}{2}}\right). \tag{17}
 \end{aligned}$$

For the irregular hexagons the following approximations are used for $i = 2, 5$

$$\begin{aligned}
 u_{h,\tau,P_i}^{k+1} + u_{h,\tau,P_i}^k &= \frac{h^2}{2\tau\omega} u_{h,\tau,P_A}^{k+1} + \frac{8}{3}u_{h,\tau,P_A}^{k+1} - u_{h,\tau,P_0}^{k+1} - \frac{1}{3}u_{h,\tau,P_{i-1}}^{k+1} \\
 &\quad - \frac{1}{3}u_{h,\tau,P_{i+1}}^{k+1} - \frac{h^2}{2\tau\omega} u_{h,\tau,P_A}^k + \frac{8}{3}u_{h,\tau,P_A}^k - u_{h,\tau,P_0}^k \\
 &\quad - \frac{1}{3}u_{h,\tau,P_{i-1}}^k - \frac{1}{3}u_{h,\tau,P_{i+1}}^k + \frac{h^2b}{4\omega} \left(u_{h,\tau,P_A}^{k+1} + u_{h,\tau,P_A}^k\right) \\
 &\quad - \frac{h^2}{2\omega} f_{P_A}^{k+\frac{1}{2}} + O(h^4 + h^2\tau^2). \tag{18}
 \end{aligned}$$

$$\begin{aligned}
 u_{h,\tau,P_i}^{k+1} - u_{h,\tau,P_i}^k &= -u_{h,\tau,P_0}^{k+1} - \frac{1}{3}u_{h,\tau,P_{i+1}}^{k+1} - \frac{1}{3}u_{h,\tau,P_{i-1}}^{k+1} \\
 &\quad + \frac{8}{3}u_{h,\tau,P_A}^{k+1} + u_{h,\tau,P_0}^k + \frac{1}{3}u_{h,\tau,P_{i-1}}^k + \frac{1}{3}u_{h,\tau,P_{i+1}}^k \\
 &\quad - \frac{8}{3}u_{h,\tau,P_A}^k + \frac{h^2b}{4\omega} \left(u_{h,\tau,P_A}^{k+1} - u_{h,\tau,P_A}^k \right) \\
 &\quad - \frac{h^2}{4\omega} \left(f_{P_A}^{k+1} - f_{P_A}^k \right) + O(h^4 + h^2\tau). \tag{19}
 \end{aligned}$$

Hence, the scheme (10) is obtained by substituting (18) and (19) in (17). Consequently, the error function $\varepsilon_{h,\tau} = u_{h,\tau} - u$ satisfies the next difference problem

$$\Theta_{h,\tau}^1 \varepsilon_{h,\tau}^{k+1} = \Lambda_{h,\tau}^1 \varepsilon_{h,\tau}^k + \Psi_1^k \text{ on } D^{0h}\gamma_\tau, \tag{20}$$

$$\Theta_{h,\tau}^2 \varepsilon_{h,\tau}^{k+1} = \Lambda_{h,\tau}^2 \varepsilon_{h,\tau}^k + \Psi_2^k \text{ on } D^{*h}\gamma_\tau, \tag{21}$$

$$\varepsilon_{h,\tau} = 0 \text{ on } t = 0, \overline{D^h}, \tag{22}$$

$$\varepsilon_{h,\tau} = 0 \text{ on } S_T^h, \tag{23}$$

where

$$\Psi_1^k = \Lambda_{h,\tau}^1 u^k - \Theta_{h,\tau}^1 u^{k+1} + \psi^1, \tag{24}$$

$$\Psi_2^k = \Lambda_{h,\tau}^2 u^k - \Theta_{h,\tau}^2 u^{k+1} + E_{h,\tau} \phi + \psi^2, \tag{25}$$

and ψ^1, ψ^2 are as given in (13), (14) respectively. Using Taylor's expansion around the point $(x_1, x_2, t + \frac{\tau}{2})$ we obtain $\Psi_1^k = O(h^4 + \tau^2)$ and $\Psi_2^k = O(h^4 + \tau^2)$.

Next, we analyze the stability for the special scheme in HDP. At every time stage using standard ordering the hexagon points in $D^h\gamma_\tau$ are labeled as $E_j, j = 1, 2, \dots, N$. Thus, all hexagon centers have the neighboring topology denoted by the following set

$$S_E = \{(i, j) : \text{if the grid } E_i \in \text{Patt}(E_j), i \neq j, 1 \leq i, j \leq N\}, \tag{26}$$

exhibiting the sparsity structure of $Inc \in R^{N \times N}$ called the incidence matrix with entries

$$[Inc]_{ij} = \begin{cases} 0 & \text{if } (i, j) \notin S_E, \\ 1 & \text{if } (i, j) \in S_E. \end{cases}$$

Further, the scheme in HDP can be put in the subsequent matrix form

$$K_1 U^{k+1} = K_2 U^k + \tau F^{k*}, \tag{27}$$

where, $K_1, K_2 \in R^{N \times N}$ are given as

$$K_1 = \left(S_1 + \frac{\omega\tau}{h^2} S_2 \right), \quad K_2 = \left(S_1 - \frac{\omega\tau}{h^2} S_2 \right), \tag{28}$$

$$S_1 = D_1 + \frac{1}{24} Inc, \quad S_2 = B + \frac{bh^2}{\omega} C, \tag{29}$$

$$B = D_2 - \frac{1}{3} Inc, \quad C = D_3 + \frac{1}{48} Inc. \tag{30}$$

Also the computed values of f in (13), (14) and the values of φ and ϕ in HDP (9)–(12) are presented by the vector $F^{k*} \in R^N$. Further, D_1, D_2, D_3 are diagonal matrices with entries

$$[D_1]_{jj} = \begin{cases} \frac{3}{4} & \text{if } E_j \in D^{0h}\gamma_\tau \\ \frac{17}{24} & \text{if } E_j \in D^{*h}\gamma_\tau \end{cases}, \quad j = 1, 2, \dots, N,$$

$$[D_2]_{jj} = \begin{cases} 2 & \text{if } E_j \in D^{0h}\gamma_\tau \\ \frac{7}{3} & \text{if } E_j \in D^{*h}\gamma_\tau \end{cases}, \quad j = 1, 2, \dots, N,$$

$$[D_3]_{jj} = \begin{cases} \frac{3}{8} & \text{if } E_j \in D^{0h}\gamma_\tau \\ \frac{17}{48} & \text{if } E_j \in D^{*h}\gamma_\tau \end{cases}, \quad j = 1, 2, \dots, N,$$

accordingly. The stiffness matrix K_1 at the $(k+1)$ th time level and the coefficient matrix K_2 at the k th time level both have 7 nonzero diagonals. Next we analyze the properties of the derived matrices.

Lemma 1. a) S_1 in (29) and the matrices B and C in (30) are SPD matrices. b) K_1 in (28) and S_2 in (29) are SPD matrices.

Proof. a) Using (26) if $E_i \in \text{Patt}(E_j)$ for $i \neq j$, $1 \leq i, j, \leq N$ this implies that $E_j \in \text{Patt}(E_i)$ giving $\text{Inc}^T = \text{Inc}$. Thus, S_1, B , and C are real symmetric matrices hence the eigenvalues of S_1, B , and C are real. Hexagonal grid is connected grid in the rectangle D thus, by using (30) it can be easily shown that the matrix B has positive diagonal entries, *i.e.* $b_{ii} > 0$, $i = 1, \dots, N$ and it is irreducibly diagonally dominant matrix. Further, the matrices S_1 , and C also have positive diagonal entries and are strictly diagonally dominant matrices [27] therefore, S_1, B and C are SPD matrices. b) From (29), since the sum of two SPD matrices is also an SPD matrix, S_2 and K_1 are SPD matrices.

Theorem 2. The constructed scheme HDP on hexagon system of grids is stable for any $h > 0$ and $\tau > 0$ and the approximate solution $u_{h,\tau}$ converges to the exact solution u with $O(h^4 + \tau^2)$ of accuracy on the hexagonal grids.

Proof. From Lemma 1, the matrix S_1 is an SPD matrix hence invertible. The linear system (27) can be written as

$$\left(I + \frac{\omega\tau}{h^2} (S_1)^{-1} S_2\right) U^{k+1} = \left(I - \frac{\omega\tau}{h^2} (S_1)^{-1} S_2\right) U^k + \tau (S_1)^{-1} F^{k*}, \quad (31)$$

where $I \in R^{N \times N}$ is the identity matrix. On the other hand using (28)–(30) we can express the matrices S_1, C and S_2 as linear combination of the identity matrix I and the matrix B as:

$$S_1 = I - \frac{1}{8}B, \quad C = \frac{1}{2}I - \frac{1}{16}B, \quad S_2 = \frac{1}{2} \frac{bh^2}{\omega} I + \left(1 - \frac{1}{16} \frac{bh^2}{\omega}\right) B. \quad (32)$$

Because $(S_1)^{-1} S_2$ commutes and S_1 and S_2 are symmetric implies that $(S_1)^{-1} S_2$ is also a symmetric matrix. Since the product of two SPD matrices that commute is also an SPD matrix [27, 28] gives $\lambda_s \left((S_1)^{-1} S_2 \right) > 0$. Let $A = \left(I + \frac{\omega\tau}{h^2} (S_1)^{-1} S_2 \right)$ obviously A is an SPD matrix. Let $\hat{A} = \left(I - \frac{\omega\tau}{h^2} (S_1)^{-1} S_2 \right)$.

$$\begin{aligned} (A^{-1}\hat{A})^T &= \hat{A}A^{-1} = \left(I - \frac{\omega\tau}{h^2} (S_1)^{-1} S_2 \right) \left(I + \frac{\omega\tau}{h^2} (S_1)^{-1} S_2 \right)^{-1} \\ &= \frac{1}{\det \left(I + \frac{\omega\tau}{h^2} (S_1)^{-1} S_2 \right)} \left(I - \frac{\omega\tau}{h^2} (S_1)^{-1} S_2 \right) \text{Adj} \left(I + \frac{\omega\tau}{h^2} (S_1)^{-1} S_2 \right) \\ &= \left(I + \frac{\omega\tau}{h^2} (S_1)^{-1} S_2 \right)^{-1} \left[I - \frac{1}{\det \left(I + \frac{\omega\tau}{h^2} (S_1)^{-1} S_2 \right)} \left(I + \frac{\omega\tau}{h^2} (S_1)^{-1} S_2 \right) \right. \\ &\quad \left. \left(\frac{\omega\tau}{h^2} (S_1)^{-1} S_2 \right) \text{Adj} \left(I + \frac{\omega\tau}{h^2} (S_1)^{-1} S_2 \right) \right] \\ &= \left(I + \frac{\omega\tau}{h^2} (S_1)^{-1} S_2 \right)^{-1} \left(I - \frac{\omega\tau}{h^2} (S_1)^{-1} S_2 \right) = A^{-1}\hat{A}. \end{aligned} \quad (33)$$

Thus $A^{-1}\hat{A}$ is a symmetric matrix, then there exists an orthogonal matrix \tilde{P} and a diagonal matrix \tilde{D} with diagonal entries of eigenvalues $\lambda_s \left((S_1)^{-1} S_2 \right)$ so that

$$\left(I + \frac{\omega\tau}{h^2} (S_1)^{-1} S_2 \right) = \tilde{P}^T \left(I + \frac{\omega\tau}{h^2} \tilde{D} \right) \tilde{P},$$

and

$$\left(I + \frac{\omega\tau}{h^2} (S_1)^{-1} S_2\right)^{-1} = \tilde{P}^T \left(I + \frac{\omega\tau}{h^2} \tilde{D}\right)^{-1} \tilde{P}.$$

Thus,

$$\left(I + \frac{\omega\tau}{h^2} (S_1)^{-1} S_2\right)^{-1} \left(I - \frac{\omega\tau}{h^2} (S_1)^{-1} S_2\right) = \tilde{P}^T \left(I + \frac{\omega\tau}{h^2} \tilde{D}\right)^{-1} \tilde{P} \tilde{P}^T \left(I - \frac{\omega\tau}{h^2} \tilde{D}\right) \tilde{P},$$

that is, the matrix $A^{-1}\hat{A}$ is similar to $\left(I + \frac{\omega\tau}{h^2} \tilde{D}\right)^{-1} \left(I - \frac{\omega\tau}{h^2} \tilde{D}\right)$. Hence, from (33)

$$\begin{aligned} \left\|A^{-1}\hat{A}\right\|_2 &= \rho\left(A^{-1}\hat{A}\right) = \max_{1 \leq s \leq N} \left| \lambda_s \left[\left(I + \frac{\omega\tau}{h^2} \tilde{D}\right)^{-1} \left(I - \frac{\omega\tau}{h^2} \tilde{D}\right) \right] \right| \\ &\leq \left| \frac{1 - \frac{\omega\tau}{h^2} \min_{1 \leq s \leq N} (\lambda_s ((S_1)^{-1} S_2))}{1 + \frac{\omega\tau}{h^2} \min_{1 \leq s \leq N} (\lambda_s ((S_1)^{-1} S_2))} \right| < 1 \text{ for } \frac{\omega\tau}{h^2} > 0 \end{aligned} \quad (34)$$

and from Gerchgorin's circle theorem we have

$$0 < \lambda_s(B) \leq 4. \quad (35)$$

From (32) and (35) and on the basis of Lemma 1 that $K_1 = S_1 + \frac{\omega\tau}{h^2} S_2$ is an SPD matrix we have

$$\begin{aligned} K_1 &= \left(1 + \frac{1}{2}\tau b\right) I + \left(-\frac{1}{8} + \frac{\omega\tau}{h^2} - \frac{b\tau}{16}\right) B \\ \lambda_s(K_1) &= \lambda_s\left(S_1 + \frac{\omega\tau}{h^2} S_2\right) \\ &= \left(1 + \frac{1}{2}\tau b\right) + \left(-\frac{1}{8} + \frac{\omega\tau}{h^2} - \frac{b\tau}{16}\right) \lambda_s(B) \\ \rho\left((K_1)^{-1}\right) &= \rho\left(\left(S_1 + \frac{\omega\tau}{h^2} S_2\right)^{-1}\right) = \left\|\left(S_1 + \frac{\omega\tau}{h^2} S_2\right)^{-1}\right\|_2 \leq \frac{1}{\varkappa}, \end{aligned}$$

where $\varkappa = \min\left\{1 + \frac{1}{2}\tau b, \frac{1}{2} + \frac{1}{2}b\tau + \frac{4\omega\tau}{h^2}\right\}$, then

$$\left\|(K_1)^{-1}\right\|_2 \leq \frac{1}{\varkappa} < 2. \quad (36)$$

Next using (34) and (36) by induction results,

$$\begin{aligned} \left\|U^{k+1}\right\|_2 &\leq \left\|A^{-1}\hat{A}\right\|_2 \left\|U^k\right\|_2 + \tau \left\|(K_1)^{-1}\right\|_2 \left\|F^{k*}\right\|_2 \\ &\leq \left\|U^0\right\|_2 + 2 \sum_{k'=0}^k \tau \left\|F^{k'*}\right\|_2. \end{aligned} \quad (37)$$

The error function $\varepsilon_{h,\tau}$ satisfying (20)–(23) can also be given in the matrix form (31) as

$$\left(I + \frac{\omega\tau}{h^2} (S_1)^{-1} S_2\right) \epsilon^{k+1} = \left(I - \frac{\omega\tau}{h^2} (S_1)^{-1} S_2\right) \epsilon^k + \tau (S_1)^{-1} \hat{\Psi}^{k*}, \quad (38)$$

where $\epsilon^{k+1}, \epsilon^k$ and $\hat{\Psi}^{k*} \in R^N$ and $\hat{\Psi}^{k*}$ involves the truncation errors given in (24), (25). Thus, on the basis of Theorem 1 and using (24), (25) and (37), (38) we obtain

$$\left\|\epsilon^{k+1}\right\|_2 \leq 2 \sum_{k'=0}^k \tau \left\|\hat{\Psi}^{k'*}\right\|_2 \leq c_1 (h^4 + \tau^2). \quad (39)$$

Here, c_1 is a positive constant independent of h and τ . The matrix $A^{-1}\widehat{A}$ is a normal matrix since it is also a symmetric real matrix. The inequality in (34) is sufficient as well as necessary for stability from the Von Neuman condition for stability [29]. Therefore, the unconditional stability of the implicit scheme (9), (10) follows from (37). Let $\left\| \varepsilon_{h,\tau}^{k+1} \right\|_C = \frac{1}{D^h \gamma_\tau \cap \{t=(k+1)\tau\}} \max \left| \varepsilon_{h,\tau}^{k+1} \right| = \left\| \epsilon^{k+1} \right\|_\infty$, then by using (39) and norm concordance we get

$$\left\| \varepsilon_{h,\tau}^{k+1} \right\|_C \leq \left\| \epsilon^{k+1} \right\|_2 \leq c_1 (h^4 + \tau^2).$$

Therefore, the order of accuracy of the approximate solution $u_{h,\tau}$ to the exact solution u is $O(h^4 + \tau^2)$.

3 Incomplete block matrix factorization and preconditioning of an SPD-BT matrix

In this section, for a real block matrix $K \in R^{N \times N}$ of block size $n \times n$, the inequality $K \succeq_s 0$ defines that K is symmetric positive semi-definite (SPSD) matrix and $K \succ_s 0$ denotes that K is a symmetric positive definite (SPD) matrix. Analogously, $A \succeq_s B$ ($A \succ_s B$) denotes $A - B \succeq_s 0$ ($A - B \succ_s 0$). Further, for a symmetric matrix K , $\lambda_k(K)$ denotes the k th eigenvalue of K ordered in increasing order and λ_{min} and λ_{max} are the minimum and maximum eigenvalues respectively.

3.1 Block incomplete decomposition algorithm and analysis

We consider symmetric positive definite block tridiagonal (SPD-BT) matrix

$$K = \begin{bmatrix} K_{1,1} & K_{1,2} & \cdots & 0 \\ K_{2,1} & K_{2,2} & K_{2,3} & \vdots \\ \vdots & \ddots & \ddots & K_{n-1,n} \\ 0 & \cdots & K_{n,n-1} & K_{n,n} \end{bmatrix}, \tag{40}$$

of $n \times n$, block size. Additionally, the nonzero blocks may be dense and $K_{p,q}$ is of size $n_p \times n_q$ ($1 \leq n_p, n_q \leq n$) which includes the case where all or some $K_{p,q}$ are scalar entries of K and main diagonal blocks $K_{p,p}$ are square matrices. We consider approximate factorization of $K = LU - Q$ in block matrix form of a lower block triangular matrix L and an upper block triangular matrix U . We repartition the matrix K into 2×2 block form and initially for $s = 1$, take $K^{(1)} = K$

$$K^{(s)} = \begin{bmatrix} K_{1,1}^{(s)} & K_{1,2}^{(s)} \\ K_{2,1}^{(s)} & K_{2,2}^{(s)} \end{bmatrix}, \tag{41}$$

where $K_{1,1}^{(s)}$ is the current pivot and $K_{i,j}^{(s)}$ is of order $n_i^{(s)} \times n_j^{(s)}$ for $i, j = 1, 2$ and $n_2^{(s)} \gg n_1^{(s)}$, also $n_1^{(s)} = n_s$ for $s = 1, 2, \dots, n$.

For M -matrices the two-step iterative method for approximating the pivoting diagonal block inverses with rate of convergence 33 was given in [24]. Algorithm 1 approximates the inverse of the pivoting diagonal block matrix of a block tridiagonal matrix $K \succ_s 0$, analogous to the two-step iterative method in [24] however, is modified in the choice of the initial approximate inverse $Z_0^{(s)}$ at every stage s . Further, Algorithm 2 gives incomplete block factorization of a SPD-BT matrix K , (see also [27] for incomplete block decomposition techniques of matrices with special structure).

Algorithm 1. Modified two-step iterative method (MTSIM) for approximate matrix inversion.

Require: The predescribed accuracy $\varepsilon > 0$.

Ensure: I is the identity matrix and $m_s = 0, 1, \dots$, is the iteration at stage s . Also,

$$\begin{aligned} R_{m_s}^{(s)} &= I - K_{1,1}^{(s)} Z_{m_s}^{(s)} \text{ and } \Omega(R_{m_s}^{(s)}) = R_{m_s}^{(s)} + \left(R_{m_s}^{(s)}\right)^2, \\ \Psi(R_{m_s}^{(s)}) &= \left(R_{m_s}^{(s)}\right)^2 + \left(R_{m_s}^{(s)}\right)^4 \text{ and } \Gamma(R_{m_s}^{(s)}) = \left(R_{m_s}^{(s)}\right)^4. \end{aligned}$$

1. Initial step

$$\begin{aligned} &\text{Step1(I)} \\ \beta^{(s)} &= \lambda_{max} \left(K_{1,1}^{(s)} \left(K_{1,1}^{(s)} \right)^T \right) \\ m_s &= 0, Z_0^{(s)} = \frac{\left(K_{1,1}^{(s)} \right)^T}{\beta^{(s)}}, \text{ and } R_0^{(s)} = I - K_{1,1}^{(s)} Z_0^{(s)}. \end{aligned}$$

2. Prediction and correction steps:

While $\left\| R_{m_s}^{(s)} \right\|_{\infty} \leq \varepsilon < 1$ do

$$\begin{aligned} &\text{Step2(P)} \\ Z_{m_s+\frac{1}{2}}^{(s)} &= Z_{m_s}^{(s)} \left[I + \Omega(R_{m_s}^{(s)}) \right], \\ R_{m_s+\frac{1}{2}}^{(s)} &= I - K_{1,1}^{(s)} Z_{m_s+\frac{1}{2}}^{(s)}, \\ &\text{Step2(C)} \\ Z_{m_s+1}^{(s)} &= Z_{m_s+\frac{1}{2}}^{(s)} \left[I + \Omega \left(R_{m_s+\frac{1}{2}}^{(s)} \right) \left[I + \Psi \left(R_{m_s+\frac{1}{2}}^{(s)} \right) \left[I + \Gamma \left(R_{m_s+\frac{1}{2}}^{(s)} \right) \right] \right] \right], \\ R_{m_s+1}^{(s)} &= I - K_{1,1}^{(s)} Z_{m_s+1}^{(s)}, \text{ increase } m_s \text{ by one.} \end{aligned}$$

End while.

3. Terminating step: $Z^{(s)}$ denotes the matrix $Z_{m_s}^{(s)}$ obtained for performing m_s^* iterations.

Algorithm 2. Incomplete block matrix factorization of $K \succ_s 0$.

Require: $s = 1$ and $K^{(1)} = K$.

1. Partition $K^{(s)}$ as in (41).

2. While $s \leq n$ do

find the approximate inverse $Z^{(s)}$ of $K_{1,1}^{(s)}$ using the Algorithm 1.

Ensure: $\widehat{K}^{(s)}$ is an approximation of $K^{(s)}$ factored as

$$\widehat{K}^{(s)} = L^{(s)} U^{(s)} = \begin{bmatrix} I & 0 \\ K_{2,1}^{(s)} Z^{(s)} & I \end{bmatrix} \begin{bmatrix} K_{1,1}^{(s)} & K_{1,2}^{(s)} \\ 0 & K^{(s+1)} \end{bmatrix},$$

where, $K^{(s+1)} = K_{2,2}^{(s)} - K_{2,1}^{(s)} Z^{(s)} K_{1,2}^{(s)}$.

4. End while.

5. The matrix L in the final approximate factorization of K is block lower triangular matrix with diagonal blocks being identity matrix and the s th column of its lower triangular part is formed by $K_{2,1}^{(s)} Z^{(s)}$.

6. The matrix U is block upper triangular with block diagonal matrix $\{K_{1,1}^{(1)}, K_{1,1}^{(2)}, \dots, K_{1,1}^{(n)}\}$ and the s th row of its upper triangular part is formed by $K_{1,2}^{(s)}$.

Lemma 2. Let K be an SPD-BT matrix and $K_{1,1}^{(s)}$ be the pivoting diagonal block at stage s of the Algorithm 2. If $K_{1,1}^{(s)} \succ_s 0$, then $R_{m_s}^{(s)} \succeq_s 0$ for every $m_s = 0, 1, \dots$, and

$$\begin{aligned} \rho\left(R_0^{(s)}\right) &< 1, \\ R_{m_s+1}^{(s)} &= \left(R_0^{(s)}\right)^{33^{m_s+1}}, \end{aligned}$$

where $\rho\left(R_0^{(s)}\right)$ is the spectral radius of $R_0^{(s)} = I - K_{1,1}^{(s)}Z_0^{(s)}$.

Proof. For $m_s = 0$ we have $R_0^{(s)} = I - K_{1,1}^{(s)}Z_0^{(s)} = I - \frac{1}{\beta^{(s)}}K_{1,1}^{(s)}\left(K_{1,1}^{(s)}\right)^T$ and if $K_{1,1}^{(s)} \succ_s 0$, it follows that $R_0^{(s)}$ is symmetric matrix and

$$\begin{aligned} \lambda_k\left(R_0^{(s)}\right) &= 1 - \frac{1}{\beta^{(s)}}\lambda_k\left(K_{1,1}^{(s)}\left(K_{1,1}^{(s)}\right)^T\right), \\ 0 &\leq \lambda_k\left(R_0^{(s)}\right) = 1 - \frac{\lambda_k\left(\left(K_{1,1}^{(s)}\right)^2\right)}{\lambda_{\max}\left(\left(K_{1,1}^{(s)}\right)^2\right)} < 1, \end{aligned}$$

which gives $\rho\left(R_0^{(s)}\right) < 1$ and $R_0^{(s)} \succeq_s 0$. Further, from Step2(P) we get

$$\begin{aligned} R_{m_s+\frac{1}{2}}^{(s)} &= I - K_{s,s}^{(s)}Z_{m_s}^{(s)}\left[I + R_{m_s}^{(s)} + \left(R_{m_s}^{(s)}\right)^2\right] \\ &= \left(R_{m_s}^{(s)}\right)^3. \end{aligned} \quad (42)$$

Also from the Step2(C) in Algorithm 1 using (42) we get

$$\Omega\left(R_{m_s+\frac{1}{2}}^{(s)}\right) = R_{m_s+\frac{1}{2}}^{(s)} + \left(R_{m_s+\frac{1}{2}}^{(s)}\right)^2 = \left(R_{m_s}^{(s)}\right)^3 + \left(R_{m_s}^{(s)}\right)^6, \quad (43)$$

$$\Psi\left(R_{m_s+\frac{1}{2}}^{(s)}\right) = \left(R_{m_s+\frac{1}{2}}^{(s)}\right)^2 + \left(R_{m_s+\frac{1}{2}}^{(s)}\right)^4 = \left(R_{m_s}^{(s)}\right)^6 + \left(R_{m_s}^{(s)}\right)^{12}, \quad (44)$$

$$\Gamma\left(R_{m_s+\frac{1}{2}}^{(s)}\right) = \left(R_{m_s+\frac{1}{2}}^{(s)}\right)^4 = \left(R_{m_s}^{(s)}\right)^{12}. \quad (45)$$

Using (42)–(45) at the Step2(C) for the residual error $R_{m_s+1}^{(s)}$ we obtain

$$\begin{aligned} R_{m_s+1}^{(s)} &= I - K_{s,s}^{(s)}Z_{m_s+1}^{(s)} \\ &= I - K_{s,s}^{(s)}Z_{m_s+\frac{1}{2}}^{(s)}\left[I + \Omega\left(R_{m_s+\frac{1}{2}}^{(s)}\right)\left[I + \Psi\left(R_{m_s+\frac{1}{2}}^{(s)}\right)\left[I + \Gamma\left(R_{m_s+\frac{1}{2}}^{(s)}\right)\right]\right]\right] \\ &= \left(R_{m_s}^{(s)}\right)^{33} = \left(R_0^{(s)}\right)^{33^{m_s+1}}. \end{aligned}$$

Thus, $R_{m_s+1}^{(s)} \succeq_s 0$ because $R_0^{(s)} \succeq_s 0$.

Theorem 3. Let K be an SPD-BT matrix and $K^{(s)}$ be the matrix obtained at stage s of the Algorithm 2. If $K_{1,1}^{(s)} \succ_s 0$ then

$$K_{1,1}^{(s)}Z_{m_s+\frac{1}{2}}^{(s)} = Z_{m_s+\frac{1}{2}}^{(s)}K_{1,1}^{(s)}, \text{ and } K_{11}^{(s)}Z_{m_s+1}^{(s)} = Z_{m_s+1}^{(s)}K_{1,1}^{(s)}, \quad (46)$$

and $Z_{m_s+\frac{1}{2}}^{(s)} \succ_s 0$, and $Z_{m_s+1}^{(s)} \succ_s 0$ satisfying

$$\left(K_{1,1}^{(s)}\right)^{-1} \succeq_s Z_{m_s+1}^{(s)} \succeq_s Z_{m_s+\frac{1}{2}}^{(s)} \succeq_s Z_{m_s}^{(s)} \succ_s 0, \tag{47}$$

for every $m_s = 0, 1, \dots$, where $Z_{m_s+\frac{1}{2}}^{(s)}$ and $Z_{m_s+1}^{(s)}$ are the approximate inverse of $K_{1,1}^{(s)}$ obtained by Step2(P) and Step2(C) in Algorithm 1.

Proof. The proof of (46) follows from induction. Using Algorithm 1 for $m_s = 0$ and from Step1(I) gives $Z_0^{(s)} = \frac{1}{\beta^{(s)}} \left(K_{1,1}^{(s)}\right)^T$. Since $K_{1,1}^{(s)}$ is a symmetric matrix we get

$$K_{1,1}^{(s)} Z_0^{(s)} = K_{1,1}^{(s)} \frac{1}{\beta^{(s)}} \left(K_{1,1}^{(s)}\right)^T = \frac{1}{\beta^{(s)}} \left(K_{1,1}^{(s)}\right)^T K_{1,1}^{(s)} = Z_0^{(s)} K_{1,1}^{(s)}.$$

Assume that the proposition is true for m_s that is $K_{1,1}^{(s)} Z_{m_s}^{(s)} = Z_{m_s}^{(s)} K_{1,1}^{(s)}$ then for m_s+1 at the Step2(P) gives

$$\begin{aligned} K_{1,1}^{(s)} Z_{m_s+\frac{1}{2}}^{(s)} &= K_{1,1}^{(s)} Z_{m_s}^{(s)} \left[I + R_{m_s}^{(s)} + \left(R_{m_s}^{(s)}\right)^2 \right] \\ &= Z_{m_s}^{(s)} \left[I + R_{m_s}^{(s)} + \left(R_{m_s}^{(s)}\right)^2 \right] K_{1,1}^{(s)} \\ &= Z_{m_s+\frac{1}{2}}^{(s)} K_{1,1}^{(s)}. \end{aligned} \tag{48}$$

Also using (42)–(45) and (48) at the Step2(C) gives the second equation in (46).

The proof of (47) also can be given using induction. For $m_s = 0$ from Step1(I) gives $Z_0^{(s)} = \frac{1}{\beta^{(s)}} \left(K_{1,1}^{(s)}\right)^T$ and from the assumption $K_{1,1}^{(s)} \succ_s 0$ implies that $Z_0^{(s)} \succ_s 0$. Assume that the proposition is true for m_s that is $Z_{m_s}^{(s)} \succ_s 0$ then from Lemma 2 using that $R_{m_s}^{(s)} \succeq_s 0$ at the Step2(P) and using (46) gives

$$\begin{aligned} \left(Z_{m_s+\frac{1}{2}}^{(s)}\right)^T &= \left[I + R_{m_s}^{(s)} + \left(R_{m_s}^{(s)}\right)^2 \right]^T \left(Z_{m_s}^{(s)}\right)^T \\ &= Z_{m_s}^{(s)} \left[I + R_{m_s}^{(s)} + \left(R_{m_s}^{(s)}\right)^2 \right] = Z_{m_s+\frac{1}{2}}^{(s)}. \end{aligned} \tag{49}$$

Next using (42)–(45) and (49) at the Step2(C) and from (46) results

$$\begin{aligned} \left(Z_{m_s+1}^{(s)}\right)^T &= \left[I + \Omega \left(R_{m_s+\frac{1}{2}}^{(s)}\right) \left[I + \Psi \left(R_{m_s+\frac{1}{2}}^{(s)}\right) \left[I + \Gamma \left(R_{m_s+\frac{1}{2}}^{(s)}\right) \right] \right] \right]^T \left(Z_{m_s+\frac{1}{2}}^{(s)}\right)^T \\ &= Z_{m_s+1}^{(s)}. \end{aligned} \tag{50}$$

From (49) and (50) we conclude that $Z_{m_s+\frac{1}{2}}^{(s)}$ and $Z_{m_s+1}^{(s)}$ are also symmetric for m_s+1 and from Step2(P) and Step2(C) we get $Z_{m_s+\frac{1}{2}}^{(s)} \succ_s 0$ and $Z_{m_s+1}^{(s)} \succ_s 0$. Further from (46) $Z_{m_s}^{(s)} R_{m_s}^{(s)}$ and $Z_{m_s}^{(s)} \left(R_{m_s}^{(s)}\right)^2$ are symmetric matrices. Thus, yields $Z_{m_s}^{(s)} R_{m_s}^{(s)} \succeq_s 0$ and $Z_{m_s}^{(s)} \left(R_{m_s}^{(s)}\right)^2 \succeq_s 0$. From the Step2(P) results

$$\begin{aligned} \lambda_k \left(Z_{m_s+\frac{1}{2}}^{(s)} - Z_{m_s}^{(s)} \right) &= \lambda_k \left(Z_{m_s}^{(s)} R_{m_s}^{(s)} + Z_{m_s}^{(s)} \left(R_{m_s}^{(s)}\right)^2 \right) \\ &\geq \lambda_k \left(Z_{m_s}^{(s)} R_{m_s}^{(s)} \right) + \lambda_{\min} \left(Z_{m_s}^{(s)} \left(R_{m_s}^{(s)}\right)^2 \right) \geq 0 \end{aligned}$$

giving $Z_{m_s+\frac{1}{2}}^{(s)} \succeq_s Z_{m_s}^{(s)}$. Analogously, using (42)-(45) at the Step2(C) results $Z_{m_s+1}^{(s)} \succeq_s Z_{m_s+\frac{1}{2}}^{(s)}$. Denoting the error by $E_{m_s}^{(s)} = \left(K_{1,1}^{(s)}\right)^{-1} - Z_{m_s}^{(s)}$ at sth stage from $K_{1,1}^{(s)} \succ_s 0$ we get $\left(K_{1,1}^{(s)}\right)^{-1} \succ_s 0$ and using that $Z_0^{(s)} \succ_s 0$ (for $m_s = 0$) we get $E_0^{(s)}$ is symmetric matrix. Further, it follows that

$$\begin{aligned} \lambda_k \left(E_0^{(s)}\right) &= \lambda_k \left(\left(K_{1,1}^{(s)}\right)^{-1} - Z_0^{(s)}\right) \geq \lambda_{\min} \left(\left(K_{1,1}^{(s)}\right)^{-1}\right) + \lambda_k \left(-Z_0^{(s)}\right) \\ &\geq \frac{1}{\sqrt{\beta^{(s)}}} - \frac{\sqrt{\beta^{(s)}}}{\beta^{(s)}} = 0. \end{aligned}$$

Thus $E_0^{(s)} \succeq_s 0$. Assume that for m_s the proposition $E_{m_s}^{(s)} \succeq_s 0$ is true then using $K_{1,1}^{(s)} E_{m_s}^{(s)} = R_{m_s}^{(s)}$ we obtain

$$\begin{aligned} \left(K_{1,1}^{(s)}\right)^{-1} - E_{m_s+1}^{(s)} &= Z_{m_s+1}^{(s)} \\ &= Z_{m_s+\frac{1}{2}}^{(s)} \left[I + \Omega \left(R_{m_s+\frac{1}{2}}^{(s)}\right) \left[I + \Psi \left(R_{m_s+\frac{1}{2}}^{(s)}\right) \left[I + \Gamma \left(R_{m_s+\frac{1}{2}}^{(s)}\right) \right] \right] \right], \\ &= \left(K_{1,1}^{(s)}\right)^{-1} - E_{m_s}^{(s)} \left(R_{m_s}^{(s)}\right)^{32}. \end{aligned}$$

From Lemma 2, $R_{m_s}^{(s)} \succeq_s 0$ and from (46)

$$\begin{aligned} E_{m_s}^{(s)} R_{m_s}^{(s)} &= R_{m_s}^{(s)} E_{m_s}^{(s)}, \\ E_{m_s}^{(s)} R_{m_s}^{(s)} \left(E_{m_s}^{(s)} R_{m_s}^{(s)}\right)^T &= E_{m_s}^{(s)} R_{m_s}^{(s)} \left(R_{m_s}^{(s)}\right)^T \left(E_{m_s}^{(s)}\right)^T \\ &= E_{m_s}^{(s)} R_{m_s}^{(s)} R_{m_s}^{(s)} E_{m_s}^{(s)} = \left(E_{m_s}^{(s)} R_{m_s}^{(s)}\right)^T E_{m_s}^{(s)} R_{m_s}^{(s)}, \end{aligned}$$

that is $E_{m_s}^{(s)} R_{m_s}^{(s)}$ is normal. Thus from Theorem 3 in [30]

$$E_{m_s+1}^{(s)} = E_{m_s}^{(s)} \left(R_{m_s}^{(s)}\right)^{32} \succeq_s 0. \quad (51)$$

Theorem 4. Let K be an SPD-BT matrix. If Algorithm 2 is used then $K^{(s)} \succ_s 0$ and the inequality (47) holds at every stage s of the recursion.

Proof. The proof follows by induction. Assume that $K \succ_s 0$ and is block tridiagonal matrix and Algorithm 2 is used. From the assumption $K^{(1)} = K$ is an SPD matrix and particularly $K_{1,1}^{(1)} \succ_s 0$, hence Theorem 3 implies that the inequalities in (47) holds true for $s = 1$. Assume that $K^{(s)} \succ_s 0$ then it follows that $K_{i,i}^{(s)} \succ_s 0$ for $i = 1, 2$ and are regular and,

$$S_i^{(s)} = K_{i,i}^{(s)} - K_{i,j}^{(s)} \left(K_{j,j}^{(s)}\right)^{-1} K_{j,i}^{(s)}, i, j = 1, 2, i \neq j, \quad (52)$$

exist and $S_i^{(s)} \succ_s 0$, $i = 1, 2$. Since $K^{(s)} \succ_s 0$ so is $\left(K^{(s)}\right)^{-1}$. Further, from Theorem 3 the approximate inverse $Z^{(s)}$ of $K_{1,1}^{(s)}$ satisfies $\left(K_{1,1}^{(s)}\right)^{-1} \succeq_s Z^{(s)}$ and $Z^{(s)} \succ_s 0$ and from Algorithm 2

$$\left(K^{(s+1)}\right)^T = \left(K_{2,2}^{(s)} - K_{2,1}^{(s)} Z^{(s)} K_{1,2}^{(s)}\right)^T = K^{(s+1)}. \quad (53)$$

Using (52) and (53) follows $K^{(s+1)} \succ_s 0$, and (47) hold true for $s + 1$.

Theorem 5. Let K be an SPD-BT matrix of $n \times n$ block size. If $K_{1,1}^{(s)}$, $s = 1, 2, \dots, n$ are the diagonal pivoting blocks of $K^{(s)}$ at stage $s = 1, 2, \dots, n$ obtained by the Algorithm 2, then the sequences $\{Z_{m_s+1}^{(s)}\}$, obtained by Algorithm 1 converge to $(K_{1,1}^{(s)})^{-1}$, $s = 1, 2, \dots, n$, respectively in Euclidean matrix norm $\|\cdot\|_2$ when $m_s \rightarrow \infty$ with 33 order of convergence and the inequality

$$\left\| (K_{1,1}^{(s)})^{-1} - Z_{m_s+1}^{(s)} \right\|_2 \leq \frac{\|R_0^{(s)}\|_2^{33m_s+1} \left\| (K_{1,1}^{(s)})^T \right\|_2}{\beta^{(s)} (1 - \|R_0^{(s)}\|_2)},$$

holds true at the s th stage.

Proof. By taking the initial approximate inverse $Z_0^{(s)} = \frac{1}{\beta^{(s)}} (K_{1,1}^{(s)})^T$ the proof is analogous to the proof of Theorem 4 in [24].

3.2 Block hybrid preconditioning of the Conjugate Gradient method

We consider the linear system $K\tilde{u} = \tilde{b}$ where, $K \succ_s 0$ is a block tridiagonal matrix of the form (40).

Theorem 6. Let K be an SPD-BT matrix of $n \times n$ block size. If $K_{1,1}^{(s)}$, $s = 1, 2, \dots, n$ are the diagonal pivoting blocks of $K^{(s)}$ at stage $s = 1, 2, \dots, n$ obtained by the Algorithm 2, and $Z^{(s)}$ are the corresponding approximate inverses obtained by Algorithm 1 by performing m_s^* iterations, then $Z^{(s)}K_{1,1}^{(s)}$ are SPD matrices and

$$\kappa \left(Z^{(s)}K_{1,1}^{(s)} \right) \leq \frac{1 + \varepsilon}{1 - \varepsilon}, \tag{54}$$

where, $\kappa \left(Z^{(s)}K_{1,1}^{(s)} \right) = \left\| \left(Z^{(s)}K_{1,1}^{(s)} \right)^{-1} \right\|_2 \left\| Z^{(s)}K_{1,1}^{(s)} \right\|_2$ is the condition number of $Z^{(s)}K_{1,1}^{(s)}$ and $0 < \varepsilon < 1$ is the prescribed accuracy in Algorithm 1.

Proof. On the basis of Theorem 3, we have $K_{1,1}^{(s)}Z^{(s)} = Z^{(s)}K_{1,1}^{(s)}$ for every $s = 1, 2, \dots, n$ and $Z^{(s)} \succ_s 0$. Theorem 4 implies that $K_{1,1}^{(s)} \succ_s 0$ thus the product of two commuting symmetric positive definite matrices is also symmetric positive definite we get $Z^{(s)}K_{1,1}^{(s)} \succ_s 0$. Next, since $I - K_{1,1}^{(s)}Z^{(s)}$ is symmetric matrix and Algorithm 1 gives $\|I - K_{1,1}^{(s)}Z^{(s)}\|_\infty \leq \varepsilon$, yielding

$$\rho \left(I - K_{1,1}^{(s)}Z^{(s)} \right) = \left\| I - K_{1,1}^{(s)}Z^{(s)} \right\|_2 \leq \left\| I - K_{1,1}^{(s)}Z^{(s)} \right\|_\infty \leq \varepsilon < 1.$$

Therefore,

$$\left| \left\| K_{1,1}^{(s)}Z^{(s)} \right\|_2 - \|I\|_2 \right| \leq \varepsilon,$$

giving

$$1 - \varepsilon \leq \left\| K_{1,1}^{(s)}Z^{(s)} \right\|_2 \leq 1 + \varepsilon. \tag{55}$$

Also

$$\left\| \left(Z^{(s)}K_{1,1}^{(s)} \right)^{-1} \right\|_2 = \left\| \left(I - I - Z^{(s)}K_{1,1}^{(s)} \right)^{-1} \right\|_2 \leq \frac{1}{1 - \varepsilon} \tag{56}$$

so from (55) and (56) follows (54). (57)

Theorem 6 shows that $Z^{(s)}$ may be used as approximate inverse preconditioners for $K_{1,1}^{(s)}$ for $s = 1, 2, \dots, n$. Algorithm 3 gives the BHP-CG method for solving $K\tilde{u} = \tilde{b}$ based on the CG method in [25]. In this algorithm incomplete block factorization LU of K is used as implicit preconditioner while the approximate inverses $Z^{(s)}$ are used as explicit preconditioners for $K_{1,1}^{(s)}$ for $s = 1, 2, \dots, n$.

Algorithm 3. BHP-CG method.

Ensure: the construction of L and U by using the Algorithm 2.

Require: $l = 0$ and \tilde{u}_0 as an initial guess, $r_0 = \tilde{b} - K\tilde{u}_0$.

Require: p_{-1} arbitrary and $\sigma_0 = 0$.

1. While $\frac{\|r_l\|_\infty}{\|\tilde{b}\|_\infty} \leq \eta < 1$ do
2. Solve the system $LUz_l = r_l$. For the solution of the block lower triangular system $L\omega_l = r_l$ where $\omega_l = Uz_l$ forward substitution works since the diagonal blocks of L are identity matrices. Then for the solution of the block upper triangular system $Uz_l = \omega_l$, the preconditioned CG method is used to solve the block subsystems with the explicit preconditioners $Z^{(s)}$ for the matrices $K_{1,1}^{(s)}$.
3. If $l \geq 1$ then compute $\sigma_l = \langle z_l, LUz_l \rangle / \langle z_{l-1}, LUz_{l-1} \rangle$.
4. Else $\sigma_0 = 0$.
5. End if.
6. $p_l = z_l + \sigma_l p_{l-1}$ and $\alpha_l = \langle z_l, LUz_l \rangle / \langle p_l, Kp_l \rangle$,
7. $\tilde{u}_{l+1} = \tilde{u}_l + \alpha_l p_l$ and $r_{l+1} = r_l - \alpha_l Kp_l$.
8. End while.
9. Let l^* be the iteration number performed, in 1–8 then \tilde{u}_{l^*} is the approximate solution satisfying $\frac{\|r_{l^*}\|_\infty}{\|\tilde{b}\|_\infty} \leq \eta$.

4 Numerical investigation

We take $D = \{(x_1, x_2) : 0 < x_1 < 1, 0 < x_2 < \frac{\sqrt{3}}{2}\}$, for $t \in [0, 1]$ and the prescribed accuracy ε in Algorithm 1 is taken as 5×10^{-5} . Also in all tables *CPU*s stands for Central Processing Unit time in seconds and *ptl* stands for per time level wherever they appear. Let in addition, the following notations be used in this section where K_1 is the matrix in (27) and \tilde{K}_1 is as given in (8).

M_{14P}^H, M_{14P}^R denote the newly developed HDP and classical RDP.

$N^{h,\tau}(M_{14P}^H), N^{h,\tau}(M_{14P}^R)$ denote the size of the matrices K_1 and \tilde{K}_1 .

$Pre^{h,\tau}(M_{14P}^H), Pre^{h,\tau}(M_{14P}^R)$ are the preconditioning time of K_1 and \tilde{K}_1 .

$Con^{h,\tau}(M_{14P}^H), Con^{h,\tau}(M_{14P}^R)$ are the condition number of K_1 and \tilde{K}_1 .

$CT^{M_{14P}^H}, CT^{M_{14P}^R}$ denote the *CPU*s *ptl* for the method M_{14P}^H and M_{14P}^R .

$TCT^{M_{14P}^H}, TCT^{M_{14P}^R}$ denote the total *CPU*s required by the method M_{14P}^H and M_{14P}^R for solving the problem on $t \in [0, 1]$.

neg means that *CPU*s is less than one millisecond.

We present the function $\varepsilon_{h,\tau}$ defining the error on the grid points $\overline{D^h\gamma_\tau}$, by $\varepsilon^{M_{14P}^H(h,\tau)}$ obtained from the application of the method M_{14P}^H . Similarly we use $\varepsilon^{M_{14P}^R(h,\tau)}$ to show the error function $\varepsilon_{h,\tau}$ obtained by the method M_{14P}^R on the grid points $\overline{D^{h_1,h_2}\gamma_\tau}$. In addition, the convergence order of the

methods M_{14P}^H and M_{14P}^R are

$$\mathfrak{R}^{M_{14P}^H} = \log_2 \left(\frac{\left\| \varepsilon^{M_{14P}^H(2^{-\mu}, 2^{-\lambda})} \right\|_{\infty}}{\left\| \varepsilon^{M_{14P}^H(2^{-(\mu+1)}, 2^{-(\lambda+2)})} \right\|_{\infty}} \right),$$

$$\mathfrak{R}^{M_{14P}^R} = \log_2 \left(\frac{\left\| \varepsilon^{M_{14P}^R(2^{-\mu}, 2^{-\lambda})} \right\|_{\infty}}{\left\| \varepsilon^{M_{14P}^R(2^{-(\mu+1)}, 2^{-(\lambda+2)})} \right\|_{\infty}} \right),$$

respectively, where μ, λ are positive integers.

4.1 Test problem: Example 1

$$\begin{aligned} \frac{\partial u}{\partial t} &= \frac{\partial^2 u}{\partial x_1^2} + \frac{\partial^2 u}{\partial x_2^2} + f(x_1, x_2, t) \text{ on } Q_T, \\ u(x_1, x_2, 0) &= 0.07x_1^{6+\alpha} + 0.3x_2^{6+\alpha} + 1 \text{ on } \bar{D}, \\ u(x_1, x_2, t) &= v(x_1, x_2, t) \text{ on } S_T, \\ f(x_1, x_2, t) &= \left(3 + \frac{\alpha}{2}\right) t^{2+\frac{\alpha}{2}} \cos\left(t^{3+\frac{\alpha}{2}}\right) - e^{-t} \\ &\quad - (6 + \alpha)(5 + \alpha)(0.07x_1^{4+\alpha} + 0.3x_2^{4+\alpha}), \\ v(x_1, x_2, t) &= 0.07x_1^{6+\alpha} + 0.3x_2^{6+\alpha} + \sin(t^{3+\frac{\alpha}{2}}) + e^{-t}, \end{aligned}$$

where v is the exact solution. Table 2 shows the $CT^{M_{14P}^H}$, $CT^{M_{14P}^R}$ and the error norms $\left\| \varepsilon^{M_{14P}^H(h, \tau)} \right\|_{\infty}$, $\left\| \varepsilon^{M_{14P}^R(h, \tau)} \right\|_{\infty}$ for $h = 2^{-\mu}$, $\mu = 4, 5, 6, 7, 8$ when $\tau = 2^{-\lambda}$, $\lambda = 6, 8, 10, 12, 14$ and the order of convergence $\mathfrak{R}^{M_{14P}^H}$, $\mathfrak{R}^{M_{14P}^R}$ for Example 1 when $\alpha = 0.8$. Table 3 shows the same quantities by using the methods M_{14P}^H and M_{14P}^R when $\alpha = 0.01$. These tables indicate that both methods have fourth order convergence in spatial variables and second order convergence in time variable.

On the other hand the second and fifth columns of these tables show the computational time $CT^{M_{14P}^H}$ and $CT^{M_{14P}^R}$ required for the method M_{14P}^H and M_{14P}^R respectively. By analyzing the values of $CT^{M_{14P}^H}$ and $CT^{M_{14P}^R}$ we conclude that the proposed method is more economical in computational time per time level when the BHP-CG method given in Algorithm 3 is applied to solve the derived systems. This conclusion is also supported by the results given in Table 4 which demonstrates the number of grid points in the stiffness matrices $N^{h, \tau}(M_{14P}^H)$ and $N^{h, \tau}(M_{14P}^R)$, the preconditioning times $Pre^{h, \tau}(M_{14P}^H)$ and $Pre^{h, \tau}(M_{14P}^R)$, the condition numbers of the preconditioned matrices $Con^{h, \tau}(M_{14P}^H)$ and $Con^{h, \tau}(M_{14P}^R)$ and the total computational time required in seconds $TCT^{M_{14P}^H}$ and $TCT^{M_{14P}^R}$ of the methods M_{14P}^H and M_{14P}^R respectively for Example 1 when $\alpha = 0.8$.

Further, when $h = 2^{-6}$ and $\tau = 2^{-10}$ for $\alpha = 0.8$, the grid function $\left| \varepsilon^{M_{14P}^H(2^{-6}, 2^{-10})} \right|$ presenting the errors in absolute values at four time stages $t = 0.25, 0.5, 0.75, 1$ by the method M_{14P}^H are shown in Figure 3 for Example 1. Analogously, Figure 4 demonstrate the function $\left| \varepsilon^{M_{14P}^R(2^{-6}, 2^{-10})} \right|$ at the same time levels and (h, τ) pair and α value obtained by the method M_{14P}^R .

Table 2

Results by the methods M_{14P}^H and M_{14P}^R for Example 1 when $\alpha = 0.8$

(h, τ)	$CT^{M_{14P}^H}$	$\ \varepsilon^{M_{14P}^H(h,\tau)}\ _{\infty}$	$\Re^{M_{14P}^H}$	$CT^{M_{14P}^R}$	$\ \varepsilon^{M_{14P}^R(h,\tau)}\ _{\infty}$	$\Re^{M_{14P}^R}$
$(2^{-4}, 2^{-6})$	neg	$4.19389E - 5$		neg	$4.26584E - 5$	
$(2^{-5}, 2^{-8})$	0.047	$2.62266E - 6$	3.9992	0.047	$2.66787E - 6$	3.9991
$(2^{-6}, 2^{-10})$	0.156	$1.63922E - 7$	3.9999	0.234	$1.66749E - 7$	3.9999
$(2^{-7}, 2^{-12})$	0.641	$1.02449E - 8$	4.0000	1.016	$1.04224E - 8$	3.9999
$(2^{-8}, 2^{-14})$	2.578	$6.40304E - 10$	4.0000	4.312	$6.51384E - 10$	4.0000

Table 3

Results by the methods M_{14P}^H and M_{14P}^R for Example 1 when $\alpha = 0.01$

(h, τ)	$CT^{M_{14P}^H}$	$\ \varepsilon^{M_{14P}^H(h,\tau)}\ _{\infty}$	$\Re^{M_{14P}^H}$	$CT^{M_{14P}^R}$	$\ \varepsilon^{M_{14P}^R(h,\tau)}\ _{\infty}$	$\Re^{M_{14P}^R}$
$(2^{-4}, 2^{-6})$	neg	$4.19389E - 5$		neg	$2.98695E - 5$	
$(2^{-5}, 2^{-8})$	0.047	$2.62266E - 6$	3.9994	0.047	$1.86757E - 6$	3.9994
$(2^{-6}, 2^{-10})$	0.188	$1.63922E - 7$	3.9999	0.219	$1.16726E - 7$	3.9999
$(2^{-7}, 2^{-12})$	0.64	$1.02449E - 8$	4.0000	1.016	$7.29597E - 9$	3.9999
$(2^{-8}, 2^{-14})$	2.5	$6.40298E - 10$	4.0000	4.25	$4.56001E - 10$	3.9999

Table 4

Computational efficiency comparison of M_{14P}^H , M_{14P}^R for Example 1 when $\alpha = 0.8$

(h, τ)	$(2^{-4}, 2^{-6})$	$(2^{-5}, 2^{-8})$	$(2^{-6}, 2^{-10})$	$(2^{-7}, 2^{-12})$	$(2^{-8}, 2^{-14})$
$N^{h,\tau}(M_{14P}^H)$	233	977	4001	16193	65153
$N^{h,\tau}(M_{14P}^R)$	225	961	3969	16129	65025
$Pre^{h,\tau}(M_{14P}^H)$	neg	neg	0.063	0.36	2.797
$Pre^{h,\tau}(M_{14P}^R)$	neg	neg	0.062	0.359	2.625
$Con^{h,\tau}(M_{14P}^H)$	0.99997	0.99993	0.99989	0.99986	0.99983
$Con^{h,\tau}(M_{14P}^R)$	0.99991	0.99988	0.99987	0.99985	0.99981
$TCT^{M_{14P}^H}$	0.61	9.09	194.84	2659.03	42582.52
$TCT^{M_{14P}^R}$	0.70	11.83	272.91	4258.53	71073.79

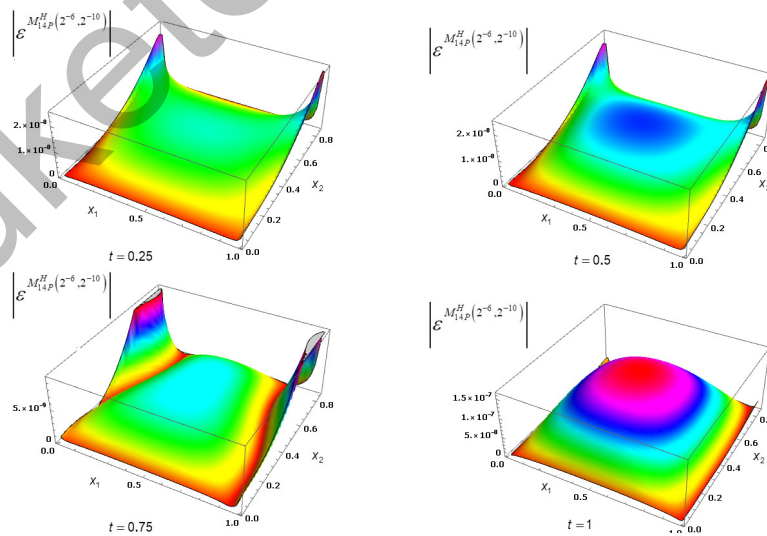


Figure 3. The grid function $|\varepsilon^{M_{14P}^H(2^{-6}, 2^{-10})}|$ when $t = 0.25, 0.5, 0.75, 1$ by M_{14P}^H for Example 1.

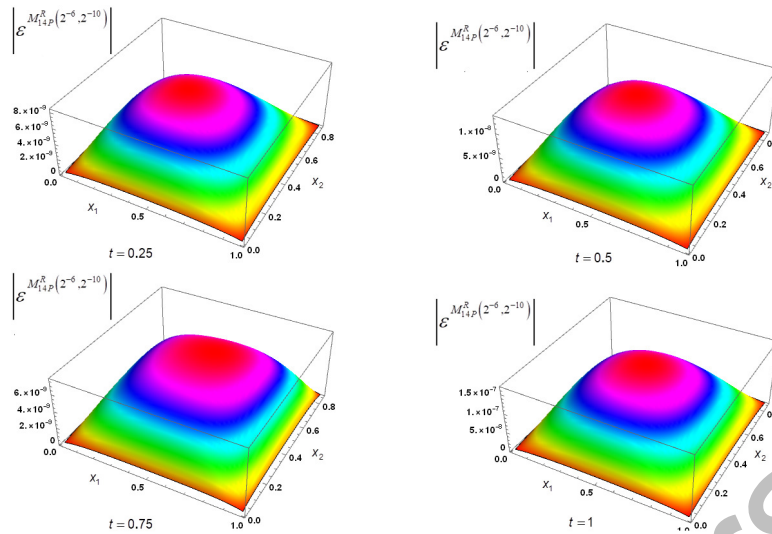


Figure 4. The grid function $\left| \mathcal{E}^{M_{14P}^R(2^{-6}, 2^{-10})} \right|$ when $t = 0.25, 0.5, 0.75, 1$ by M_{14P}^R for Example 1.

4.2 Test problem: Example 2

$$\begin{aligned} \frac{\partial u}{\partial t} &= \frac{\partial^2 u}{\partial x_1^2} + \frac{\partial^2 u}{\partial x_2^2} - 0.5u + f(x_1, x_2, t) \text{ on } Q_T, \\ u(x_1, x_2, 0) &= \frac{1}{2}x_1^{\frac{37}{6}} + x_2^{\frac{37}{6}} + 1 \text{ on } \bar{D}, \\ u(x_1, x_2, t) &= v(x_1, x_2, t) \text{ on } S_T, \\ f(x_1, x_2, t) &= -\left(\frac{37}{12}t^{\frac{25}{12}} \sin\left(t^{\frac{37}{12}}\right) + \frac{1147}{72}x_1^{\frac{25}{6}} + \frac{1147}{36}x_2^{\frac{25}{6}} \right) \\ &\quad + 0.5\left(\frac{1}{2}x_1^{\frac{37}{6}} + x_2^{\frac{37}{6}} + \cos\left(t^{\frac{37}{12}}\right) \right), \\ v(x_1, x_2, t) &= \frac{1}{2}x_1^{\frac{37}{6}} + x_2^{\frac{37}{6}} + \cos\left(t^{\frac{37}{12}}\right), \end{aligned}$$

where, v is the exact solution. Table 5 demonstrates the $CT^{M_{14P}^H}$, $TCT^{M_{14P}^H}$ and the error norms for $h = 2^{-\mu}$, $\mu = 4, 5, 6, 7, 8$ when $\tau = 2^{-\lambda}$, $\lambda = 6, 8, 10, 12, 14$ respectively, and the order of convergence $\mathfrak{R}^{M_{14P}^H}$ for Example 2. Figure 5 shows the absolute error function $\left| \mathcal{E}^{M_{14P}^H(2^{-6}, 2^{-10})} \right|$ for time values $t = 0.25, 0.5, 0.75, 1$ obtained by the given method M_{14P}^H for Example 2.

Table 5

Results by the method M_{14P}^H for Example 2

(h, τ)	$CT^{M_{14P}^H}$	$TCT^{M_{14P}^H}$	$\left\ \mathcal{E}^{M_{14P}^H(h, \tau)} \right\ _{\infty}$	$\mathfrak{R}^{M_{14P}^H}$
$(2^{-4}, 2^{-6})$	neg	0.61	$2.378442E - 5$	
$(2^{-5}, 2^{-8})$	0.047	9.907	$1.543029E - 6$	3.9462
$(2^{-6}, 2^{-10})$	0.172	207.547	$1.015411E - 7$	3.9256
$(2^{-7}, 2^{-12})$	0.735	2904.99	$6.623985E - 9$	3.9382
$(2^{-8}, 2^{-14})$	2.829	50743	$4.251592E - 10$	3.9616

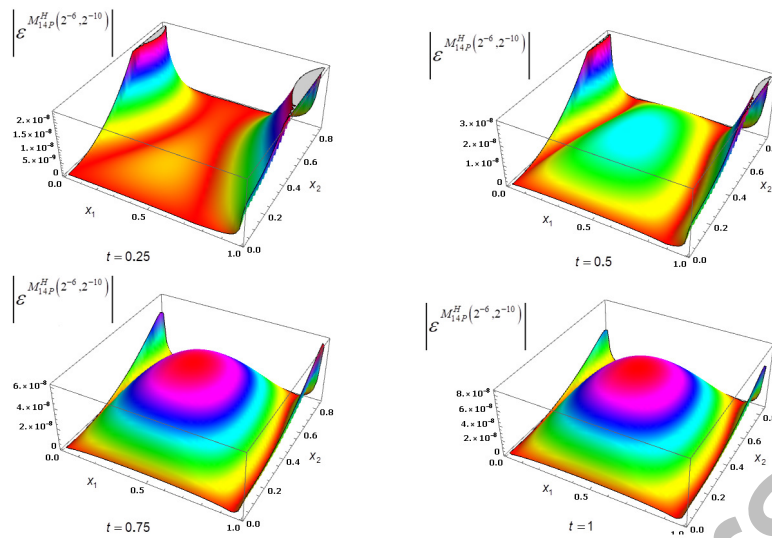


Figure 5. The grid function $\left| \mathcal{E}^{M_{14P}^H(2^{-6}, 2^{-10})} \right|$ when $t = 0.25, 0.5, 0.75, 1$ by M_{14P}^H for Example 2.

5 Conclusion

On a hexagonal system of grids, a novel implicit method is developed for approximating the solution to the DBVP of the heat equation (2)–(4) on rectangle. Further, by using the modified two-step iterative method, block hybrid preconditioning of the conjugate gradient method is given. The obtained theoretical and numerical results demonstrate that the given implicit method is economical since it is computationally time efficient. We remark that in Section 2, the given implicit scheme on hexagonal grids was studied in the dissertation [31].

References

- 1 Ashyralyev, A., & Haso, B. (2022). Stability of the time-dependent identification problem for the delay-hyperbolic equation. *International Journal of Applied Mathematics*, 35(3), 473–494.
- 2 Ashyralyev, A., & Al-Hazaimeh, H. (2022). Stability of the time-dependent identification problem for the telegraph equation with involution. *International Journal of Applied Mathematics*, 35(3), 447–459.
- 3 Ashyralyev, A., & Ashyralyev, C. (2022). On the stability of parabolic differential and difference equations with a time-nonlocal condition. *Computational Mathematics and Mathematical Physics*, 62(6), 962–973.
- 4 Ashyralyev, A., & Ashyralyev, C. (2022). Numerical solution of time-nonlocal problem for parabolic equation. *AIP Conference Proceedings*, 2483, 060001.
- 5 Buranay, S.C., & Arshad, N. (2020). Hexagonal grid approximation of the solution of heat equation on special polygons. *Advances in Difference Equations*, 2020:309, 1–24.
- 6 Buranay, S.C., Matan, A.H., & Arshad, N. (2021). Two stage implicit method on hexagonal grids for approximating the first derivatives of the solution to the heat equation. *Fractal Fract.*, 5(19), 1–26.
- 7 Buranay, S.C., Arshad, N., & Matan, A.H. (2021). Hexagonal Grid Computation of the Derivatives of the Solution to the Heat Equation by Using Fourth-Order Accurate Two-Stage Implicit Methods. *Fractal Fract*, 5(203), 1–34.

- 8 Richtmyer, R.D., & Morton, K.W. (1967). *Difference methods for initial-value problems*, second edition. Interscience Publishers a division of John Wiley and Sons.
- 9 Sadourny, R., Arakawa, A., & Mintz, Y. (1968). Integration of the nondivergent barotropic vorticity equation with an icosahedral-hexagonal grid for the sphere. *Mon. Wea. Rev.*, 96(6), 351–356.
- 10 Williamson, D.L. (1968). Integration of the barotropic vorticity equation on a spherical geodesic grid. *Tellus*, 20, 642–653.
- 11 Sadourny, R. (1969). Numerical integration of the primitive equation on a spherical grid with hexagonal cells. *Proceedings of the WMO/IUGG Symposium on Numerical Weather Prediction, Vol. VII. WMO*, 45–77.
- 12 Sadourny, R. & Morel, P. (1969). A finite-difference approximation of the primitive equations for a hexagonal grid on a plane, *Mon. Wea. Rev.*, 97(6), 439–445.
- 13 Masuda, Y. (1969). A finite difference scheme by making use of hexagonal mesh-points. *Proceedings of the WMO/IUGG Symposium on Numerical Weather Prediction in Tokyo, 1968*. Teck.Rep. of JMA, VII35-VII44.
- 14 Masuda, Y., & Ohnishi, H. (1986). An integration scheme of the primitive equation model with an icosahedral-hexagonal grid system and its application to the shallow water equation. *Short and Medium-Range Numerical Weather Prediction, T. Matsumo Ed., Collection of Papers Presented at the WMO/IUGG Symposium on Numerical Weather Prediction*, 317–326.
- 15 Thacker, W.C. (1977). Irregular grid finite difference techniques: Simulations of oscillations in shallow circular basins. *J. Phys. Oceanogr*, 7(2), 284–292.
- 16 Ničkovič, S. (1994). On the use of hexagonal grids for simulation of atmospheric processes. *Contrib. Atmos. Phys.*, 67, 103–107.
- 17 Karaa, S. (2006). High-order approximation of 2D convection-diffusion equation on hexagonal grids. *Numerical Methods for Partial Differential Equations*, 22, 1238–1246.
- 18 Dosiyevev, A.A., & Celiker, E. (2014). Approximation on the hexagonal grid of the Dirichlet problem for Laplace's equation. *Boundary Value Problems*, 2014:73, 1–19.
- 19 Lee, D., Tien, H.C., Luo, C.P., & Luk, H.-N. (2014). Hexagonal grid methods with applications to partial differential equations. *International Journal of Computer Mathematics*, 91(9), 1986–2009.
- 20 Avkan, A., Nagy, B., & Saadetoğlu, M. (2020). Digitized rotations of 12 neighbors on the triangular grid. *Annals of Mathematics and Artificial Intelligence*, 88, 833–857.
- 21 Avkan, A., Nagy, B., & Saadetoğlu, M. (2022). A comparison of digitized rotations of neighborhood motion maps of closest neighbors on 2D regular grids. *Signal, Image and Video Processing*, 16, 505–513.
- 22 Dean, A., English, S., Huang, T., Krueger, R.A., Lee, A., Mizrahi, M., & Wheaton-Werle, C. (2021). Firefighting on the hexagonal grid. *Discrete Applied Mathematics*, 305, 16–22.
- 23 Liao, C., Tesfa, T., Duan, Z., & Leung, L.R. (2020). Watershed delineation on a hexagonal mesh grid. *Environmental Modelling and Software*, 128, 104702, 1–23.
- 24 Buranay, S.C., & Iyikal, O.C. (2021). Incomplete block-matrix factorization of M -matrices using two step iterative method for matrix inversion and preconditioning. *Mathematical Methods in the Applied Sciences*, 44, 7634–7650.
- 25 Concus, P., Golub, G.H., & O'Leary, D.P. (1976). *A generalized conjugate gradient method for the numerical solution of elliptic partial differential equations, in sparse matrix computations*. J.R. Bunch and D.J. Rose, eds., Academic Press, New York, 309-332.
- 26 Samarskii, A.A. (2001). *The Theory of Difference Schemes*. Marcel Dekker, Inc. New York.

- 27 Axelsson, O. (1996). *Iterative Solution Methods*. Cambridge University Press, New York.
- 28 Taussky, O. (1968). Positive-definite matrices and their role in the study of the characteristic roots of general matrices. *Advances in Mathematics*, 2(2), 175–186.
- 29 Lax, P.D., & Richtmyer, R.D. (1956). Survey of the stability of linear finite difference equations. *Communications on Pure and Applied Mathematics*, 9, 267–293.
- 30 Meenaksi, A.R., & Rajian, C. (1999). On a product of positive semidefinite matrices. *Linear Algebra and its Applications*, 295, 3–6.
- 31 Arshad, N. (2020). *Hexagonal grid approximation of the solution of two dimensional heat equation*. Doctoral thesis, Eastern Mediterranean University, Famagusta, Cyprus.

С.К. Буранай¹, Н. Ашад²

¹Шығыс Жерорта теңізі университеті, Фамагуста, Түркия;

²Рауф Денкташ университеті, Никосия, Түркия

Түйіндес градиенттер әдісін блокты-гибридті қайта шарттауға қолдана отырып, жаңа айқын емес схема бойынша жылу өткізгіштік теңдеуін шешу

Зерттеудің негізгі мақсаты – алтыбұрыштардың тор жүйесінде жаңа айырымдық әдісін жасау арқылы тіктөртбұрыштағы жылу өткізгіштік теңдеуінің Дирихле шеттік есептердің шешімін жуықтау. Бұл арнайы схема сөзсіз тұрақты және кеңістіктік айнымалылар бойынша төртінші дәлдік реті және уақыт айнымалысы бойынша екінші дәлдік реті бар торлардағы нақты шешімге жақындайтыны дәлелденді. Екіншіден, толық емес блоктық факторландыру симметриялы оң анықталған блоктық үшбұрышты матрицалар үшін симметриялы оң анықталған қасиетті сақтай отырып, айналмалы диагональды блоктардың кері жағына жуықтайтын консервативті итерациялық әдісті қолдана отырып берілген. Болашақта факторландыру блогының көмегімен алынған алгебралық теңдеулер жүйесін әр уақыт деңгейінде шешу үшін түйіндес градиенттер әдісінің гибриді қайта шарттауы қолданылады.

Кілт сөздер: жылу өткізгіштік теңдеуі, айқын емес схема, алтыбұрышты тор, тұрақтылықты талдау, симметриялы оң анықталған матрица, жуықталған кері, толық емес блокты факторландыру, блокты-гибридті қайта шарт қою, түйіндес градиенттер әдісі.

С.К. Буранай¹, Н. Ашад²

¹Восточно-средиземноморский университет, Фамагуста, Турция;

²Университет Рауфа Денкташа, Никосия, Турция

Решение уравнения теплопроводности по новой неявной схеме с использованием блочно-гибридного предобусловливания метода сопряженных градиентов

Основной целью исследования является аппроксимация решения краевой задачи Дирихле уравнения теплопроводности на прямоугольнике путем разработки нового разностного метода на сеточной системе шестиугольников. Доказано, что данная специальная схема безусловно устойчива и сходится к точному решению на сетках с четвертым порядком точности по пространственным переменным и вторым порядком точности по временной переменной. Во-вторых, неполная блочная факторизация дана для симметричных положительно определенных блочных трехдиагональных матриц с использованием консервативного итеративного метода, который аппроксимирует обратную сторону поворотных

диагональных блоков, сохраняя симметричное положительно определенное свойство. В дальнейшем с помощью этого блока факторизации применено гибридное предобуславливание метода сопряженных градиентов для решения полученной алгебраической системы уравнений на каждом временном уровне.

Ключевые слова: уравнение теплопроводности, неявная схема, гексагональная сетка, анализ устойчивости, симметричная положительно определенная матрица, приближенная обратная, неполная блочная факторизация, блочно-гибридное предобуславливание, метод сопряженных градиентов.

Букеетов Университет